

# Supplementary Materials: Bulk-Like SnO<sub>2</sub>-Fe<sub>2</sub>O<sub>3</sub>@Carbon Composite as a High-Performance Anode for Lithium Ion Batteries

Jie Deng <sup>1†</sup>, Yu Dai <sup>2†</sup>, Zhe Xiao <sup>3</sup>, Shuang Song <sup>2</sup>, Hui Dai <sup>2,4</sup>, Luming Li <sup>1,5,\*</sup> and Jing Li <sup>2,\*</sup>

- <sup>1</sup> College of Pharmacy and Biological Engineering, Chengdu University, Chengdu 610106, China; dengjie@cdu.edu.cn  
<sup>2</sup> Department of Chemical Engineering, Sichuan University, Chengdu 610065, China; daiyuscu@163.com (Y.D.); 2016323050027@stu.scu.edu.cn (S.S.); dahu18@cdut.edu.cn (H.D.)  
<sup>3</sup> Institute of New Energy and Low Carbon Technology, Sichuan University, Chengdu 610207, China; 2017226220007@stu.scu.edu.cn  
<sup>4</sup> College of Materials and Chemistry & Chemical Engineering, Chengdu University of Technology, Chengdu, 610065, China;  
<sup>5</sup> Institute of Advanced Study, Chengdu University, Chengdu 610106, China  
\* Correspondence: liluming@cdu.edu.cn (L.L.); jingli0726@g.ucla.edu (J.L.)  
† These authors contributed equally to this work.

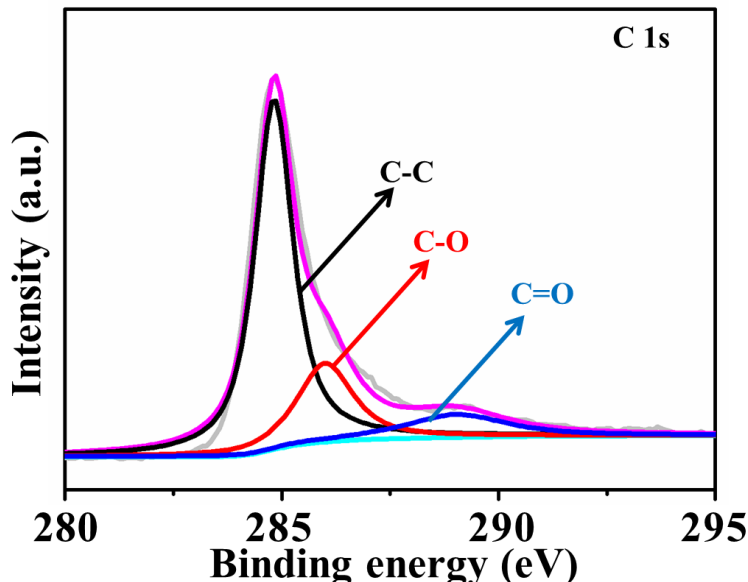


Figure S1. XPS spectra of C 1s for B-SFO@C sample.

Table S1. The weight fractions of SnO<sub>2</sub> and Fe<sub>2</sub>O<sub>3</sub> in B-SFO@C sample calculated different methods

methods	SnO <sub>2</sub>	Fe <sub>2</sub> O <sub>3</sub>
ICP	63.5%	9.2%
XPS	47.2%	7.5%

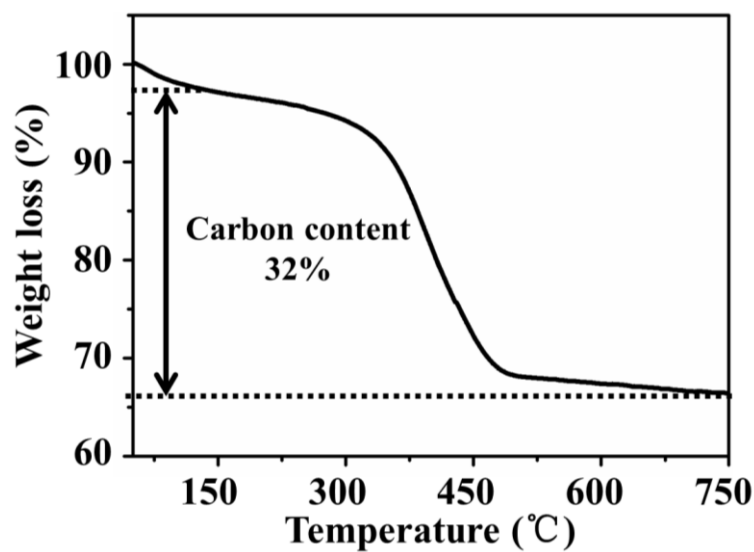


Figure S2. TGA curves of the B-SFO@C sample.

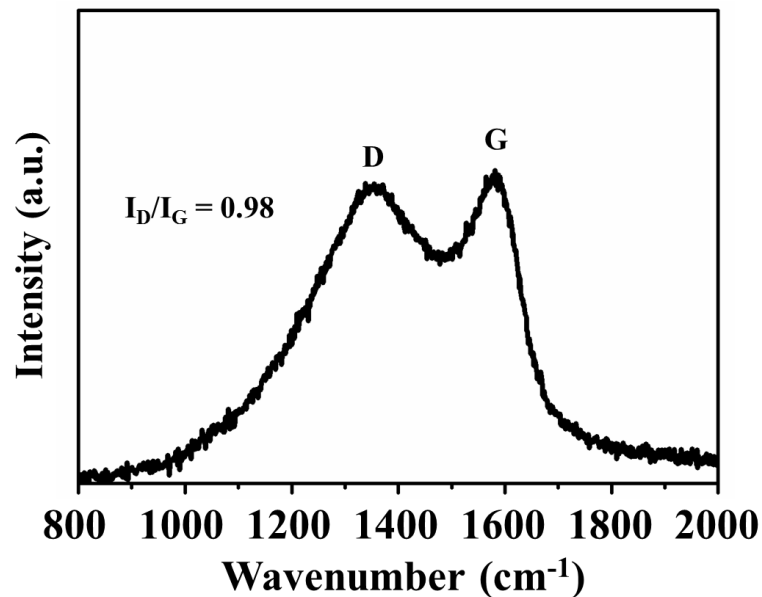
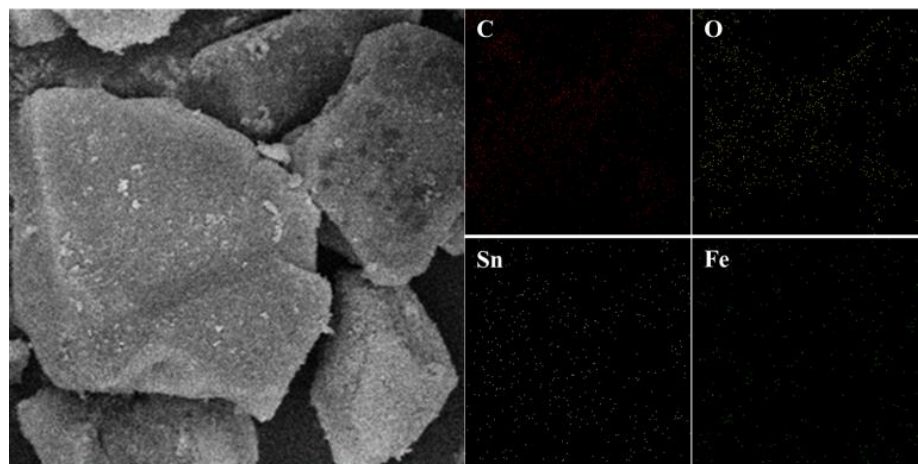
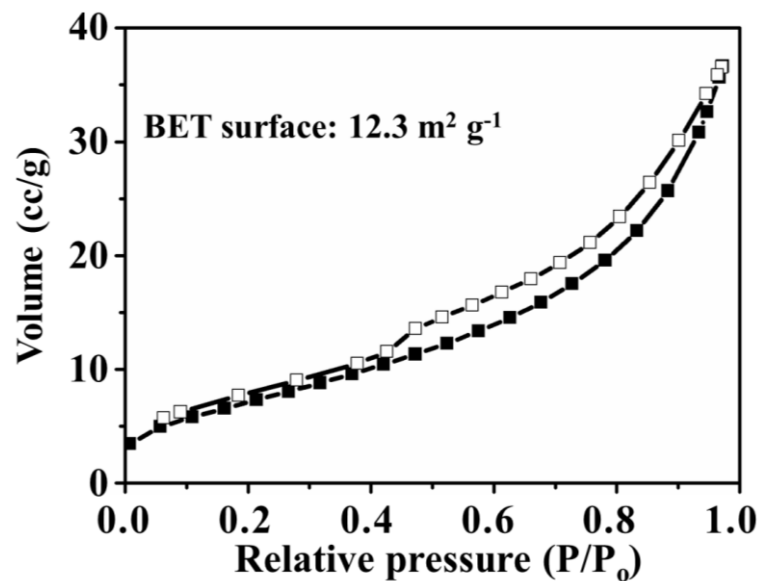


Figure S3. Raman spectrum of the B-SFO@C sample.



**Figure S4.** EDX mapping images of the B-SFO@C sample.



**Figure S5.** Nitrogen adsorption–desorption isotherms of B-SFO@C sample.

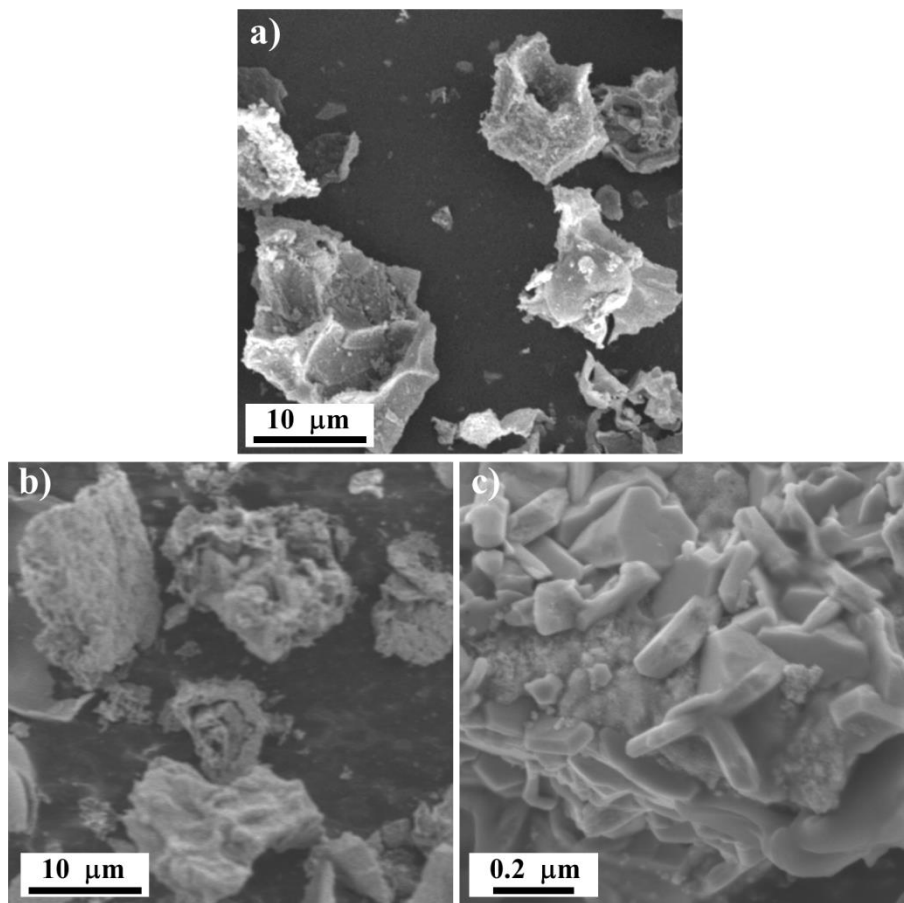


**Figure S6.** (a) SEM images of B-SO@C sample, (b) Low-resolution and (c) High-resolution SEM image of B-SFO sample.

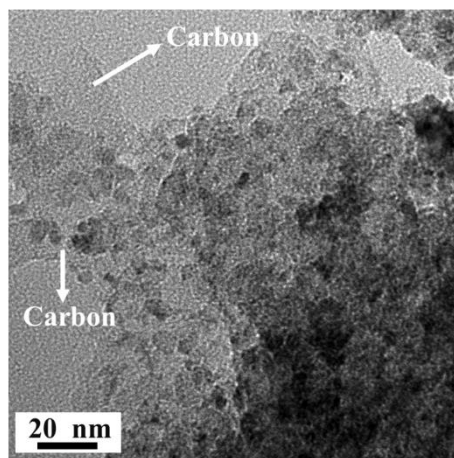


**Figure S7.** Magnified TEM image of the B-SFO@C sample.

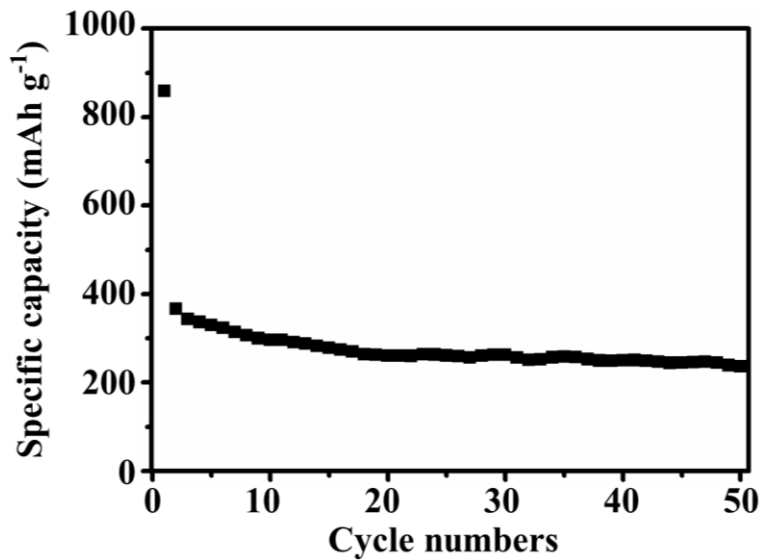


**Figure S8.** Cyclic performance of carbon matrix at  $0.2 \text{ A g}^{-1}$  in the range of  $0.005\text{--}3.0 \text{ V}$ .

**Table S2.** The electrochemical performances of B-SFO@C and SnO<sub>2</sub>-based composites anode materials in the previous reports.

Sample	Current density ( $\text{A g}^{-1}$ )	Initial coulombic efficiency	Remained Capacity ( $\text{mAh g}^{-1}$ )	Cycle number	Ref.
Bulk SnO <sub>x</sub> @C	0.2	46.3%	885.8	360	1
	1		637.2	1000	
Carbon-Encapsulated Porous SnO <sub>2</sub>	0.05	41.6%	870.9	120	2
Honeycomb-like SnO <sub>2</sub> @C	0.2	66.2%	940	150	3
	1		400	500	
SnO <sub>2</sub> @CNT	0.2	62.5%	546	100	4
	1		398	150	
3D h-SnO <sub>2</sub> -Fe <sub>2</sub> O <sub>3</sub> @RGO	0.2	61.3%	830	100	5
rGO/ Fe <sub>2</sub> O <sub>3</sub> / SnO <sub>2</sub>	0.4	63%	700	100	6
Fe <sub>2</sub> O <sub>3</sub> @SnO <sub>2</sub> /GS	0.1	60.8%	1015	200	7
SnO <sub>2</sub> /Fe <sub>2</sub> O <sub>3</sub> /RGO	0.2	46%	795	220	8
	1		690	1000	
SnO <sub>2</sub> -Fe <sub>2</sub> O <sub>3</sub> /SWCNTs	0.2	64.9%	692	50	9
	1		553	100	
B-SFO@C	0.2	70%	927	100	This work
	1		701	500	
	3		429	1800	

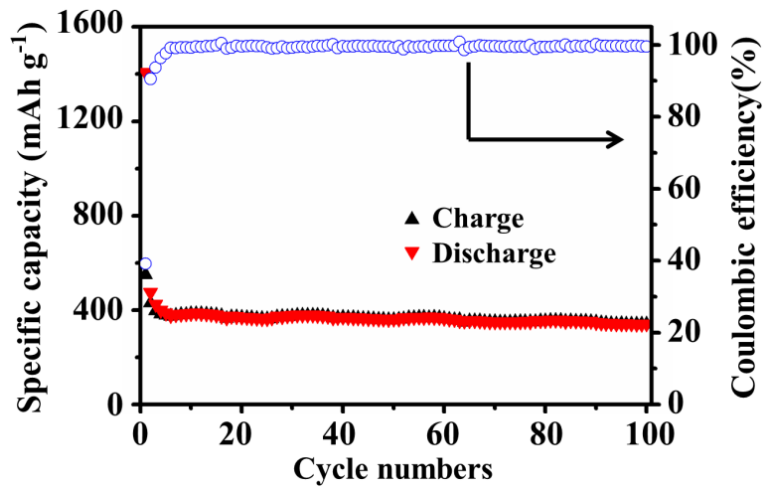


**Figure S9.** Cyclic performance of B-SFO@C electrode at 0.2 A g<sup>-1</sup> in the range of 0.005–1.0 V.

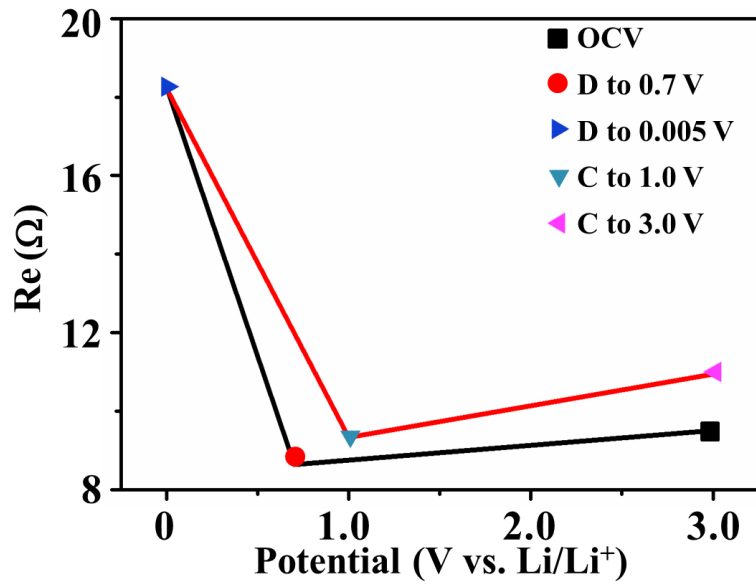


**Figure S10.** The corresponding fitted  $R_e$  at different SOC.

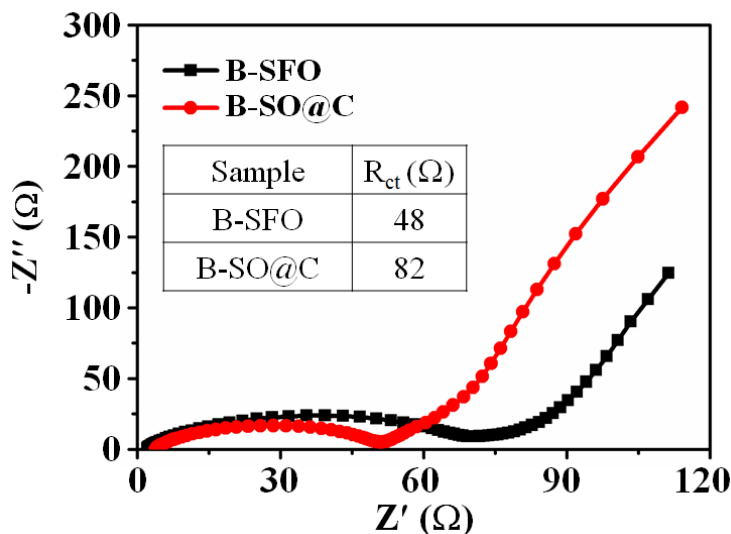


**Figure S11.** EIS spectra of fresh B-SO@C and B-SFO electrodes the corresponding fitted  $R_{ct}$  (inset).

## References

- Tian, Q.H.; Hong, Z.M.; Chen, P.; Zhang, Z. X.; Li, Y. Bulk SnO<sub>x</sub>@C composite for improved lithium storage. *J. Alloy. Compd.*, **2018**, *740*, 312–320.
- Huang, B.; Li, X.H.; Pei, Y.; Li, S.; Cao, X.; Masse, R.C., Cao, G.Z. Novel carbon-encapsulated porous SnO<sub>2</sub> anode for lithium-ion batteries with much improved cyclic stability. *Small*, **2016**, *12*, 1945–1955.
- Wang, H.K.; Wang, J.K.; Cao, D.X.; Gu, H.Y.; Li, B.B.; Lu, X.; Han, X.G.; Rogach, A.L.; Niu, C.M. Honeycomb-like carbon nanoflakes as a host for SnO<sub>2</sub> nanoparticles allowing enhanced lithium storage performance. *J. Mater. Chem. A*, **2017**, *5*, 6817–6824.
- Cheng, Y.Y.; Huang, J.F.; Qi, H.; Cao, L.Y.; Yang, J.; Xi, Q.; Luo, X.M.; Yanagisawa, K.; Li, J.Y. Adjusting the chemical bonding of SnO<sub>2</sub>@CNT composite for enhanced conversion reaction kinetics. *Small*, **2017**, *13*, 1700656–1700666.
- Zhao, B.; Xu, Y.T.; Huang, S.Y.; Zhang, K.; Yuen, M.M.F.; Xu, J.B.; Fu, X.Z.; Sun, R.; Wong, C.P. 3D RGO frameworks wrapped hollow spherical SnO<sub>2</sub>-Fe<sub>2</sub>O<sub>3</sub> mesoporous nano-shells: fabrication, characterization and lithium storage properties. *Electrochim. Acta*, **2016**, *202*, 186–196.
- Xia, G.F.; Li, N.; Li, D.Y.; Liu, R.Q.; Wang, C.; Li, Q.; Lu, X.J.; Spendelow, J.S.; Zhang, J.L.; Wu, G. Graphene/Fe<sub>2</sub>O<sub>3</sub>/SnO<sub>2</sub> ternary nanocomposites as a high-performance anode for lithium ion batteries. *ACS Appl. Mater. Interfaces*, **2013**, *5*, 8607–8614.
- Liu, S.; Wang, R.H.; Liu, M.M.; Luo, J.Q.; Jin, X.H.; Sun, J.; Gao, L. Fe<sub>2</sub>O<sub>3</sub>@SnO<sub>2</sub> nanoparticle decorated graphene flexible films as high-performance anode materials for lithium-ion batteries. *J. Mater. Chem. A*, **2014**, *2*, 4598–4604.
- Lee, K.; Shin, S.; Degen, T.; Lee, W.; Yoon, Y.S. In situ analysis of SnO<sub>2</sub>/Fe<sub>2</sub>O<sub>3</sub>/RGO to unravel the structural collapse mechanism and enhanced electrical conductivity for lithium-ion batteries. *Nano Energy*, **2017**, *32*, 397–407.
- Wu, W.L.; Zhao, Y.; Li, J.X.; Wu, C.X.; Guan, L.H. A ternary phased SnO<sub>2</sub>-Fe<sub>2</sub>O<sub>3</sub>/SWCNTs nanocomposite as a high-performance anode material for lithium ion batteries. *J. Energy Chem.*, **2014**, *23*, 376–382.